Women in Aerospace

University of Illinois at Urbana-Champaign

Team Mentors: Jonathan Sivier and Mark Joseph

Faculty Adviser: Diane Jeffers (dejeffer@illinois.edu)

Team Lead: Alexandra Bacula (bacula2@illinois.edu)

Katherine Carroll

Ian Charter

Melanie Ciancio

Sara Kochanski

Sara Legg

Christopher Lorenz

Lui Suzuki

May 27 , 2016

TABLE OF CONTENTS

TABLE OF FIGURES

TABLE OF TABLES

1. Rocket Operation Assessment

1.1. Flight Anomalies Analysis

The first flight of the rocket (with active drag disabled) was a very stable flight and there were no anomalies during launch other than the lack of camera footage. Although the camera was secure and turned on prior to launch, by the time the rocket took off from the launch pad the keychain camera battery had drained, meaning that the first flight was not caught on camera. On the second flight (intended to be with active drag), the drag fins never deployed. This was confirmed via the altimeter readings as well as the onboard video camera footage. After inspection of the active drag components, the source of the problem was determined to be that the SD card, used for the storage of the altimeter data from our custom system, had fallen out. Without this SD card, the program controlling the active drag deployment was stuck in a loop searching for the SD card, so it never started analyzing altitude data and therefore did not trigger active drag deployment. This was rectified for the third flight by the addition of a piece of tape to secure the SD card in place. Finally, on the third flight (the second attempt at using the active drag) the drag fins deployed properly after motor burnout and retracted before apogee, as intended. The fins caused a small amount of wobble to the flight path, as expected. Despite this, the overall flight path was straight. There was an anomaly during descent, and the main parachute did not deploy. This will be further discussed in Section 1.4 Recovery Analysis, below.

1.2. Summary of Flight Characteristics

Three tables explaining the characteristics of each flight are provided below. Information on the weight of the rocket, the motor used, its peak altitude, maximum velocity and acceleration, and average coefficient of drag with respect to each flight are given in the tables below.

Table 1. Flight Characteristics of first flight, no active drag

Weight on pad	19.3 lbs
Motor	Cesaroni K500
Apogee	3491 ft (Stratologger) 1052 m [3451 ft] (AltimeterTwo)
Maximum Velocity	584.5 ft/s
Maximum Acceleration	213.81 ft/s^2
Average coefficient of drag (during time active drag fins would be deployed)	0.185

Table 2. Flight Characteristics of second flight, no active drag

Weight on pad	19.3 lbs
Motor	Cesaroni K500
Apogee	3457 ft (Stratologger) 1054 m [3458 ft] (AltimeterTwo)
Maximum Velocity	506.7 ft/s
Maximum Acceleration	235.89 ft/s^2
Average coefficient of drag (during time active drag fins would be deployed)	0.176

Table 3. Flight Characteristics of third flight, with active drag

Weight on pad	19.3 lbs
Motor	Cesaroni K500
Apogee	2679 ft (Stratologger) 819 m [2687 ft] (AltimeterTwo)
Maximum Velocity	562.34 ft/s
Maximum Acceleration	268.64 ft/s^2
Average coefficient of drag (during time active drag fins were deployed)	0.88

1.3. Propulsion System Assessment

The propulsion system for each flight worked as expected. There was concern going into the launch of the second flight that the motor may not have as much thrust as the first one because the second motor was seven years old. However, at launch it appeared to have the same performance as the first motor. This was confirmed in the flight data which revealed that the second flight went to about the same apogee as the first flight. The only downside of using the older motor was that it was not ignited on the first attempt. A second, more powerful igniter was then used to ignite the motor. Because the reason the motor did not ignite is not known for certain, the motor cannot be definitively blamed for the lack of ignition.

1.4. Flight Path Assessment

The flight paths for all three launches were as expected, with the rocket going almost straight up on each launch. On the second launch the rocket veered into the wind slightly due to the rocket being marginally overstable, but it still travelled mainly straight up and reached an altitude 2 meters higher than the first launch. On the third launch the rocket travelled straight up, similar to the first launch. However, due to the deployment of the active drag fins, the rocket had a slight wobble about its longitudinal axis. However, this only occurred when the active drag fins were deployed, which was after motor burnout and before apogee. Photos of the third launch and flight can be seen in Figure 1.

Figure 1. Stills from the third flight of the rocket.

1.5. Recovery Analysis

The recovery for the first two flights went as planned: the drogue parachute was ejected at apogee and the main parachute was ejected at 500 ft AGL. Both ejection charges were set off by the Stratologger. For the first flight, the descent rate after the drogue parachute deployed was 69.7 ft/s and it landed at 19.8 ft/s after the main parachute deployed. During the second flight, the descent rate after the drogue parachute deployed was 67.6 ft/s and 19.6 ft/s after the main parachute deployed. During the third flight, the drogue parachute deployed at apogee; however, the main parachute did not deploy at all. Post flight analysis shows that the most likely reason the main did not deploy was due to a short somewhere in the system. This was determined by analyzing the data recorded by the Stratologger, which showed that the voltage recorded was zero only when it tried to fire the main igniter. Visual inspection of the wiring from the igniter leads to the Stratologger and from the 9V battery to the Stratologger did not show a short in the wires, so it is believed there was a short somewhere else. Further testing in an attempt to find the exact location of the short was inconclusive. It is believed it was either in the Stratologger (this was the first flight with this particular Stratologger) or the main power switch to the Stratologger (due to water remaining from the previous landing). In the future, fully redundant recovery systems will be used for both the main parachute and the drogue, rather than the drogue alone.

1.6. Rocket Location & (Ground) Recovery Analysis

After the first flight the rocket landed very close to the launchpad, no more than 150 ft away. The rocket was fully intact outwardly, though it was later discovered the SD card recording altimeter data had fallen out on impact with the ground. This issue could have been easily fixed during the hour preparation time required before flight; however, the team did not open the coupler section to ensure the SD card placement after the first launch. After the second flight, the rocket landed a bit farther away, but still within about 1000 ft of the launch site. It landed partially in a ditch containing water. Unfortunately the coupler section, which held all the electronics, was completely submerged in water. The other sections of the rocket remained dry. After letting the water drain from the vent holes, as seen in Figure 2, the team quickly gathered the rest of the rocket to check for damage. No other damage was found.

Figure 2. Water draining from the coupler section after the second flight.

The electronics were taken out of the coupler and allowed to dry for a short time before being taken into a car and held in front of a heating vent with the heat turned all the way up to facilitate drying. Once the electronics were dry enough to safely touch, the team inspected them for damage and replaced components that were unfit to be used in flight. The Stratologger was replaced, as well as the 9V battery powering it. Even though all of the active drag electronics were submerged in water, they worked without issue after they were thoroughly dried and cleaned. Ground testing was conducted to ensure the system was in flight-ready condition. After the third flight, in which the main parachute did not deploy, the impact on landing was much harder than on the previous two flights. This impact was enough to break the upper airframe, as seen in Figure 3.

Figure 3. Upper airframe after third flight landing.

The impact was also enough to crack the coupler and bend one of the eyebolts on the bulkheads as seen in Figures 4 and 5. Two of the t-nuts for the screws that hold together the coupler and the upper airframe broke off inside the rocket upon landing. A large amount of paint also came off the nose cone. Additionally, the motor controller appeared more corroded after the third flight and stopped working due to a dislodged inductor from the impact.

Figure 4. Crack in the coupler after third launch.

Figure 5. Bent eyebolt after third launch.

1.7. Pre- & Post-Launch Procedure Assessment

The team arrived at the launch site by 8:30 AM on the morning of the launches. This enabled all members to adequately prepare the rocket before the first launch, which took place before 10:00 AM. Working under the one-hour time constraint, each team member was assigned a role to re-assemble the rocket after each launch. The steps that had to be followed for pre-launch assembly and post-launch retrieval were clearly outlined in the team's flight checklist. For instance, before the launches each team member had the unique role of either folding and packing the parachutes, folding the shock cords, preparing the recovery electronics, or cleaning the motor casing. Additionally, with the help of the team's mentors, ejection charges were measured and the motor was prepared for each launch. All team members assisted in inserting the shear pins and screws to their respective places along the exterior of the body tube, as well as attaching the camera, inserting the igniter, and turning on the necessary avionics for each flight on the launch pad. An image of a team member inserting the igniter into the motor is depicted in Figure 6.

As for post-flight inspection, the team waited for the range to be clear, then retrieved the rocket and checked for undetonated charges. After returning to the safe area, the AltimeterTwo data was recorded and removed, data and camera footage were collected, and all avionics were turned off and prepared for the next flight. Some of the team members can be seen inspecting and retrieving the rocket after landing in Figure 7. In this efficient manner, the team was able to repeatedly prepare the rocket for the next launch in approximately thirty minutes, falling under the one hour time constraint.

Figure 6. Inserting igniter into motor prior to first launch.

Figure 7. Inspecting rocket after landing and before retrieval.

2. Actual vs. Predicted Performance

2.1 Peak Altitude Comparison

For all three of the rocket's flights, data collection was attempted from both the custom data logger on the Arduino, as well as the Stratologger. Unfortunately the jolt from the first flight landing dislodged the SD card that was used to save the data from the Arduino, and this anomaly was not caught until after the second flight. Therefore, as seen in Figure 8, only the first and third flights were recorded using that system. The Stratologger, however, recorded data for all three flights, as can be seen in Figure 9.

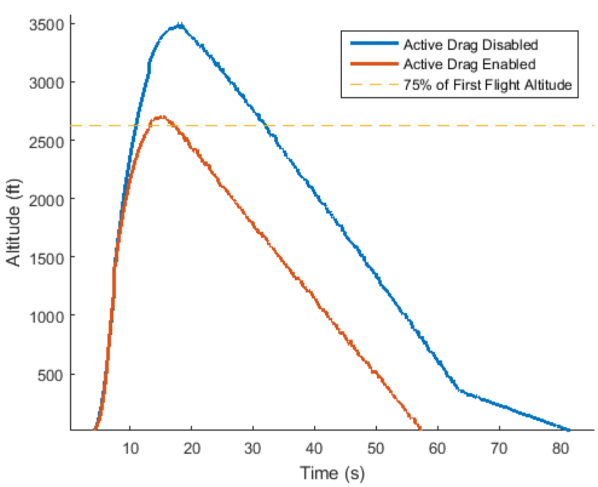

Figure 8. First flight altitude vs third flight altitude as recorded by the custom data logger.

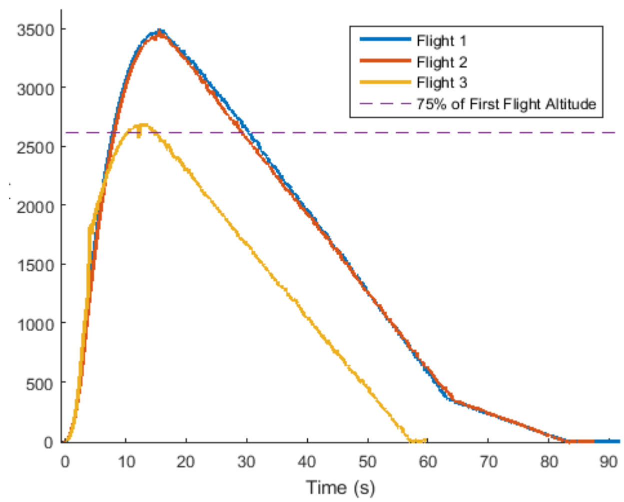

Figure 9. Altitude data collected from the Stratologger for all three flights.

The actual and predicted flight path trajectories were not identical, as can be seen in Figure 10. The simulation predicted that the rocket would go several hundred feet higher than what the rocket actually achieved. This was due to an unexpected change in the assembly of the active drag that allowed the fins to start with a slight cant. This extra area increased the overall coefficient of drag of the rocket and thus lowered the height. If the coefficient of drag is adjusted in the simulation to match the initial fin cant, as shown in Figure 11, the trajectories match much closer. Figure 11 also shows that the predicted altitude with drag would be slightly above 75 percent of the altitude without drag. This was done to account for the extra drag caused by the non-smooth paint job. After adjusting the coefficient of drag of the disabled active drag simulation to match the actual flight with the active drag disabled, it can be seen that the estimated increase in coefficient of drag from the paint was higher than expected.

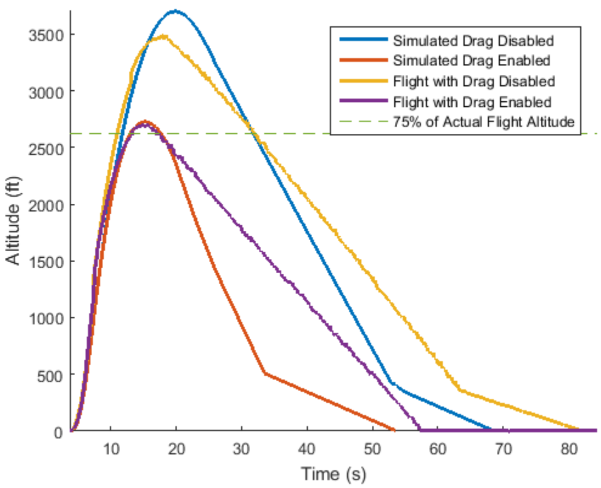

Figure 10. Initial simulation trajectory versus actual trajectory.

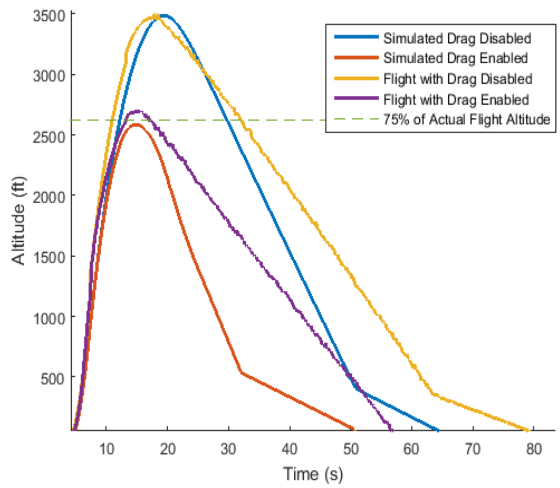

Figure 11. Adjusted simulation trajectory versus actual trajectory to account for fin cant.

2.2 Coefficient of Drag Comparison

The predicted coefficient of drag was calculated using predicted altitude data from OpenRocket and a custom MATLAB simulation. The predicted value of the coefficient of drag while the active drag fins were deployed was approximately 1.05. The actual value of the average coefficient of drag while fins were deployed in flight was 0.88, which is slightly lower than predicted, but not far off. A possible explanation for the lower value may be due to the simulation not accounting for non-ideal environmental conditions, such as a higher air density. The simulated coefficient of drag values can be seen in Figure 12.

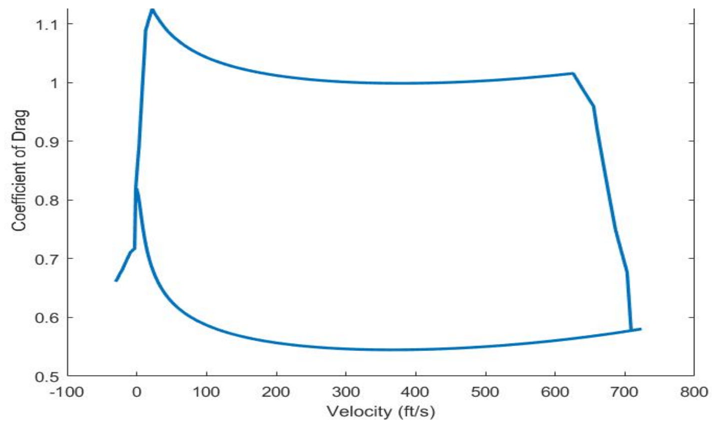

Figure 12. Custom simulation of coefficient of drag relative to velocity, with active drag.

Figure 13 shows a general decreasing trend in the coefficient of drag with respect to velocity during flight, much like the predicted plot above. Apart from the velocity range of 200 to 300 ft/s, which is around when the active drag fins were retracted, the actual values are very close to the predicted values.

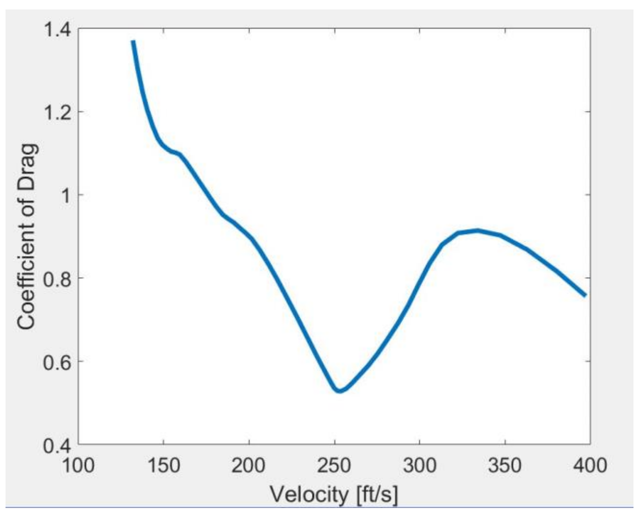

Figure 13. Coefficient of drag vs velocity during third flight, with active drag.

2.3 Peak Velocity Comparison

In both cases for the first two flights without active drag, the actual peak velocity was higher than the predicted velocity, as seen in Figures 14, 15, and 16. The predicted peak velocity was 490 ft/s, while the peak velocity of the first flight was 584.5 ft/s and the peak velocity of the second flight was 506.7 ft/s This may have been due to assuming a higher coefficient of drag for the rocket during the flights without active drag than the actual value. In the first flight, there is a second peak in the velocity plot which occurs after motor burnout. This may have been due to an anomaly in the Stratologger data, or a small error that was exacerbated during the differentiation to find velocity. If this second peak is ignored, both flights without active drag have very similar peak velocities, just above 500 ft/s.

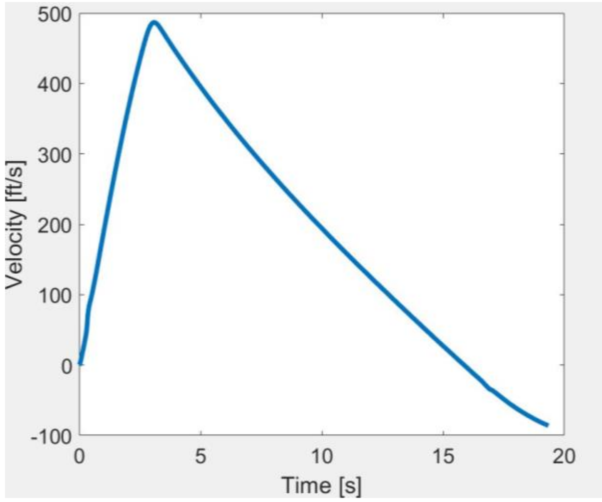

Figure 14. Predicted velocity vs time for flight without active drag.

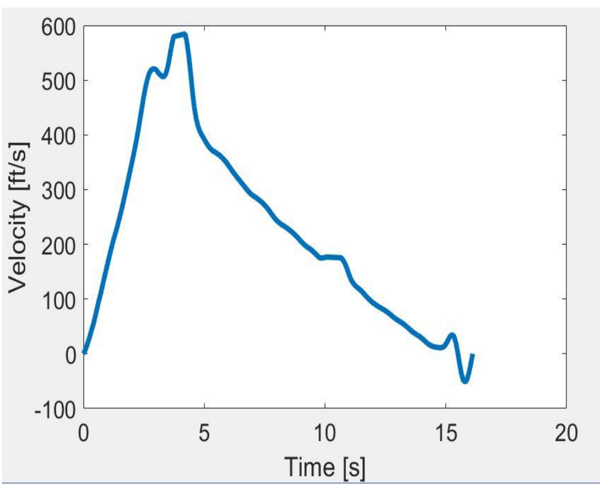

Figure 15. Actual velocity vs time of first flight, without active drag.

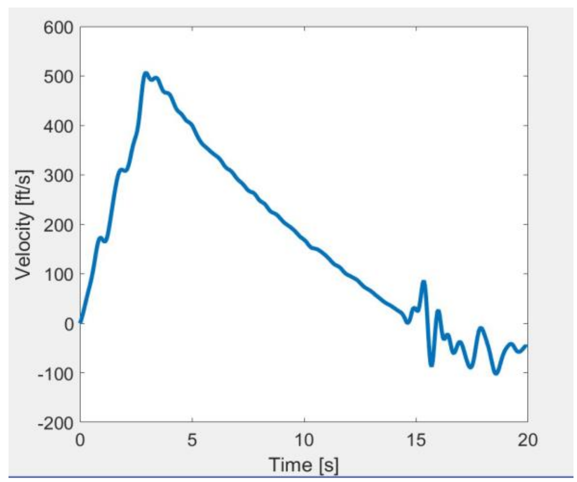

Figure 16. Actual velocity vs time of second flight, without active drag.

In the flight with the active drag, the peak velocity was also higher than predicted, as can be seen in Figures 17 and 18. The predicted peak velocity with active drag was 492.5 ft/s, while the actual peak velocity for the flight with active drag was 562.34 ft/s. A higher altitude was predicted for the active drag flight, which could account for the difference in peak velocity especially since the peak velocity was calculated by differentiating the altitude. The difference in predicted and actual altitudes could be amplified when calculating the velocity.

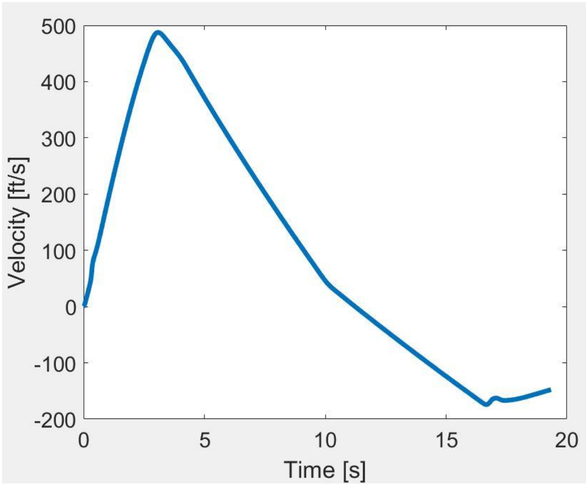

Figure 17. Predicted velocity vs time for flight with active drag.

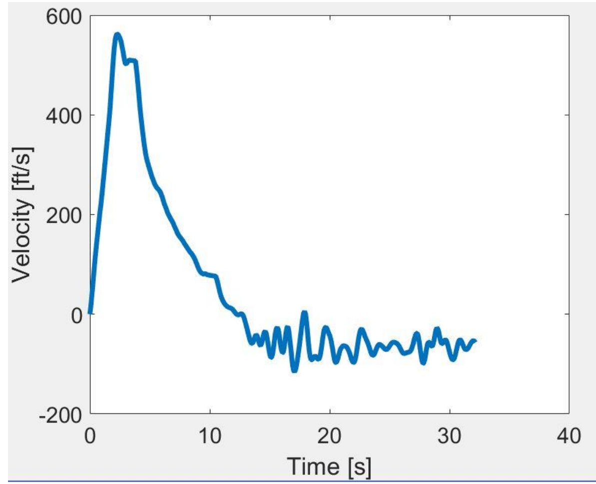

Figure 18. Actual velocity vs time for flight with active drag.

3. Data Collection

3.1 Drag System Report

The active drag fins were deployed based on an Arduino code which read altitude and time. At an altitude of 100 ft a timer started which waited 2.5 s and then began fin deployment. This 2.5 s delay was calculated to ensure the active drag did not deploy before motor burnout. At this time the Arduino also sent an output to the SD card on the Arduino that fin deployment had been triggered, so the event could be easily found in the data later. Once fin deployment was triggered, the fins turned for 0.45 s until fully opened. The fins then stayed open for 6.0 s, and then began closing for 0.65 s and returned to the stored position. During the first flight, the code still output where the fins would have been triggered, but since the actuator was intentionally not turned on the fins did not move.

Fin deployment occurred from 3.956 s after ignition until 11.056 s after ignition. The active drag fins were fully deployed from 4.046 s after ignition to 10.046 s after ignition. The exact position of the fins can be seen in Figure 19. This plot was made using data from the altimeter, responsible for triggering the active drag, to find the exact deployment and retraction times. As the fins were told to open for a set time of 0.45 s and close for a set time of 0.65 s, and because the actuator moved steadily during those time increments, the position of the active drag fins while deploying and retracting is dependent on time. This analysis is also backed up by video evidence which can be seen in Figures 20, 21, and 22. When the fins were not deployed, they were in their stored position of 20 degrees off of vertical. It is also clear that the fins deployed after motor burnout, which occurred at 3.6 s, and retracted before apogee, which occurred at 19.7 s.

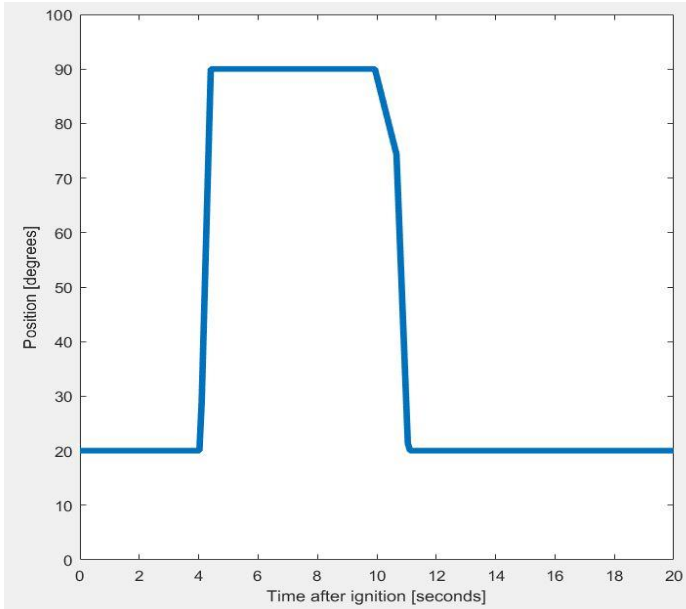

Figure 19. Position of fins vs time during flight with active drag.

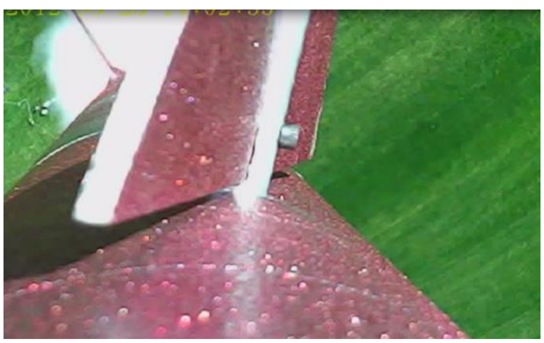

Figure 20. Active drag fins before deployment.

Figure 21. Active drag fins after deployment.

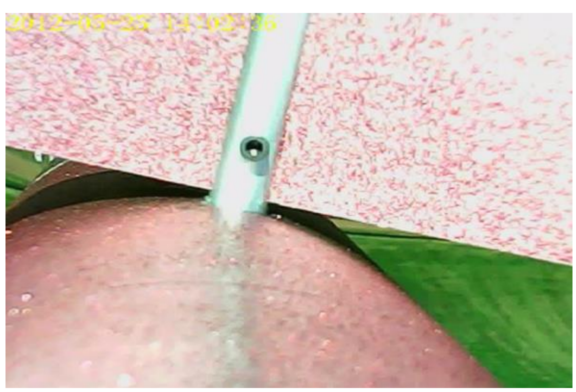

Figure 22. Active drag fins during deployment.

3.2 Coefficient of Drag Data Analysis

The coefficient of drag for the rocket was studied using the data obtained from the altimeter and Arduino used to trigger active drag deployment in the first and third flight, and data obtained from the Stratologger during the second flight. Unfortunately, the SD card saving the data from the altimeter and Arduino which triggered the active drag was not in place during the second flight, thus the Stratologger data was used. The coefficient of drag was calculated using the equation

$$C_d = 2 * F_d/(\rho u^2 A)$$

where C_d is the coefficient of drag, F_d is the force due to drag, ρ is density of air, u is the velocity of the flow, and A is the frontal area exposed to the flow. The force of drag was calculated using the mass and acceleration of the rocket. The mass of the rocket was assumed to be linearly decreasing during the burn time, and constant following motor burnout. The acceleration was calculated using an 8th order finite difference scheme over the velocity profile obtained from differentiating the altitude data acquired from the altimeter responsible for triggering the active drag system in the first and third flights. During the second flight the altitude data from the Stratologger was used. The data was smoothed using a moving average smoothing technique covering a 3.5 s range. This large smoothing range removed much of the noise from the acceleration data.

The density was calculated assuming an inverse square atmosphere from a starting density of 1.225 kg/m^2. The area assumed for the body of the rocket was calculated as the cross sectional area of the rocket body as well as bottom and deployable drag fins. This was parametrized as a function of time based on the deployment state of the fins shown in the data received from the altimeter used to trigger the active drag.

As can be seen in the figures below, the coefficient of drag was significantly higher for the flight with active drag than the flight without active drag. Near the time when active drag was initially activated, the coefficient of drag shot up as expected since area was increased. This can be compared to Figures 23 and 24, which show no drastic increase in drag at the same point in time when active drag would have been initiated. After the initial increase, the coefficient of drag plot with active drag engaged followed a similar increasing trend as the plot without active drag, just at higher values. The plot of coefficient of drag during flight versus time when active drag is engaged is depicted in Figure 26. It can be seen in comparing predicted coefficient of drag vs time and actual coefficient of drag vs time as seen in Figures 25 and 26, that the actual coefficient of drag is again very similar to the predicted and follows the same upward trend as time increases.

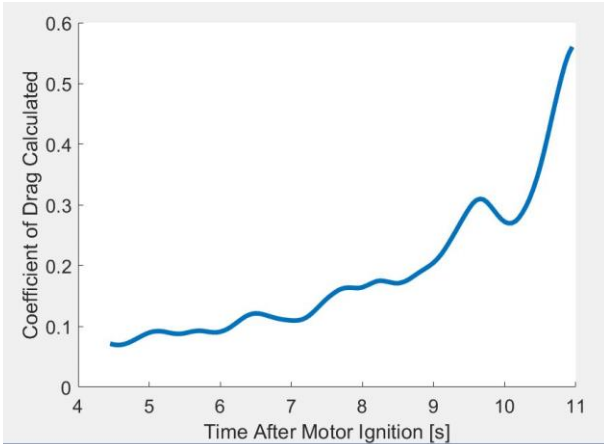

Figure 23. Coefficient of drag during first flight without active drag.

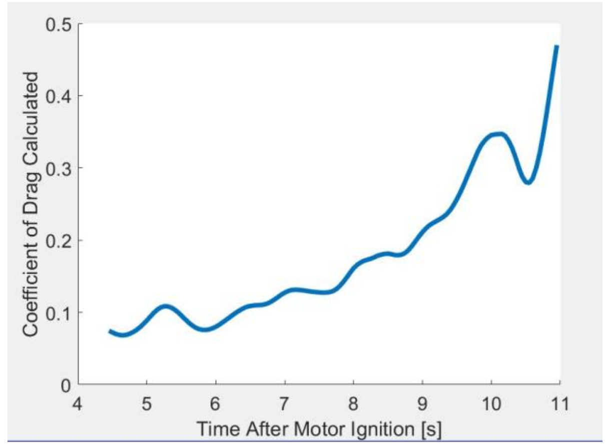

Figure 24. Coefficient of drag during second flight without active drag.

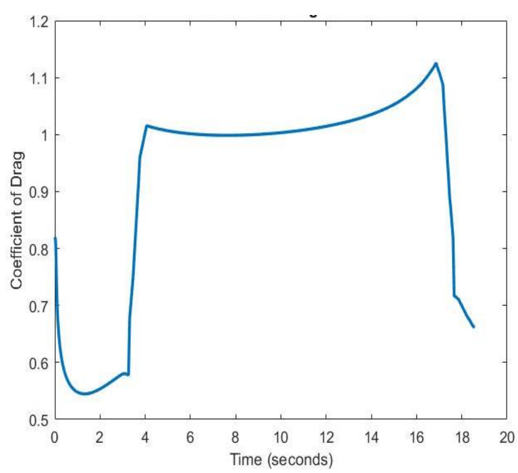

Figure 25. Predicted coefficient of drag during flight with active drag.

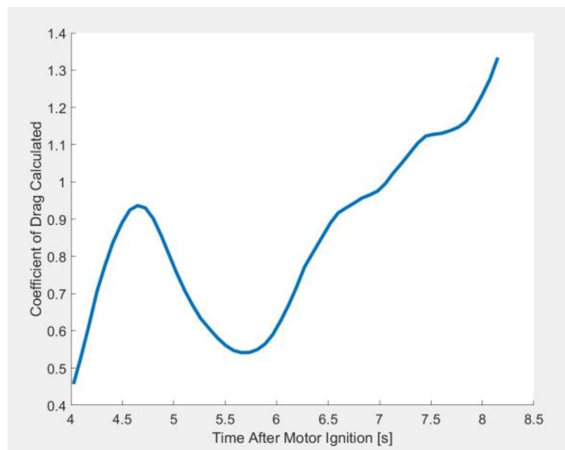

Figure 26. Actual coefficient of drag during flight with active drag.

3.3 Summary of Data Interpretation and Comparison

As described above, during the third flight with active drag engaged, the active drag fins worked as intended. The fins successfully deployed after motor burnout and retracted before apogee. Additionally, the active drag fins were initiated based on both altitude and time, which were read by Arduino code. The coefficient of drag of each flight was calculated using the force due to drag, the density of air, the velocity of the air flow, and the area exposed to the flow. These parameters were all able to be calculated and showed that with the increase in area due to the active drag fins, the coefficient of drag was increased by nearly 4.75 times the coefficient of drag of the flight without active drag. This resulted in an altitude of approximately 77 percent that of the initial flight, which is very close to the intended 75 percent goal. Thus, the active drag fins were very successful in reducing the altitude of the rocket.

The actual apogee with active drag was 2679 ft, while the predicted apogee with active drag was 2726 ft. The difference could be accounted for in that during the competition a last minute change was made to the active drag code, taking slightly longer to deploy and retract the active drag fins resulting in a slightly longer time with the active drag system in action. The predicted apogee without active drag was 3666 ft, while the actual apogee of the first flight without active drag was 3491 ft, and the actual apogee of the second flight was 3457 ft. Both actual apogees were less than the predicted apogee. A possible explanation for this is that the undeployed position of the active drag fins was not completely vertical, as assumed in the simulations, but about 20 degrees off vertical. This most likely created more drag than assumed in simulations resulting in a lower altitude.

The predicted peak acceleration for the flights without active drag was 192 ft/s^2, while the actual peak acceleration of the first flight without active drag was 213.81 ft/s^2 and the peak acceleration of the second flight without active drag was 235.89 ft/s^2. The greater acceleration may have been due to a slightly lighter rocket than used in the simulations. It may also be due to an amplified difference in peak altitudes, which were then differentiated to find the actual peak acceleration. The predicted peak acceleration for the flight with active drag was 288.84 ft/s^2, while the actual peak acceleration of the flight with active drag was 268.64 ft/s^2. The peak acceleration occurred before the active drag was activated, so the reasoning behind the larger peak acceleration in the flight without active drag should have held true for the flight with active drag, and the peak acceleration should have been much higher. The predicted acceleration for the active drag flight was calculated using a custom simulation, unlike the peak acceleration for the flights without active drag, which were calculated using OpenRocket. An anomaly in the custom simulation may account for the larger predicted acceleration. The peak acceleration is higher with the active drag than without, but it is still within an expected range.